ISME

Multiple Cracks in an Elastic Half-plane Subjected to Thermo-mechanical Loading

R. Sourki[*]
Masters Student

M. Ayatollahi[†]
Professor

M. M. Monfared[‡]
Assistant Professor

S. M.Mousavi[§]
Associate Professor

An analytical solution is presented for the thermoelastic problem of a half-plane with several cracks under thermomechanical loading using distributed dislocation technique. The uncoupled quasi-static linear thermoelasticity theory is adopted in which the change in temperature, if any, due to deformations is neglected. The stress field in a half-plane containing thermoelastic dislocation is obtained by means of the complex Fourier transform. Then, the problem is reduced to the solution of a set of simultaneous integral equations with Cauchy type singularities for dislocation density functions. Numerical results for the modes I and II stress intensity are presented to illustrate the effects of crack geometry and loading conditions on the stress intensity factors. Finally, the different cases of crack configurations and arrangements are examined.

Keywords : Thermal stress, Elastic half-plane, Thermoelastic dislocation, Multiple cracks, Stress intensity factors

1 Introduction

Many advanced engineering structures are exposed to thermal loading during their life cycles. Structural components such as advanced turbine systems, shuttles, combustion chambers and ovens operate at high temperatures, which can give rise to intense thermal stresses in these components. In particular, once a steady heat flow is disturbed by the presence of cracks, thermal stresses concentration occurs in the neighborhood of the crack tips and may lead to crack propagation. Consequently, the study of the thermal stresses in the vicinity of the crack tips is of great practical importance.

[*] Masters Student, Faculty of Engineering, University of Zanjan, Zanjan, Iran , r.sourki@gmail.com
[†]Corresponding Author, Professor, Faculty of Engineering, University of Zanjan, Zanjan, Iran, mo.ayatollahy@gmail.com
[‡] Assistant Professor, Department of Mechanical Engineering, Hashtgerd Branch, Islamic Azad University, Alborz, Iran, mo_m_monfared@yahoo.com
[§] Associate Professor, Department of Engineering and Physics, Karlstad University, 65188 Karlstad, Sweden, mahmoud.mousavi@kau.se

As an important branch in solid mechanics, the structures weakened by defects and subjected to various types of external thermomechanical loadings have been studied extensively in the literature. The thermal stresses alone or in combination with mechanical loadings can give rise to cracks and rupture in components containing brittle materials [1].Investigations concerning cracks under thermomechanical loading are briefly reviewed here. Sih [2]studied the thermoelastic fracture problem where the temperature distribution is stationary. He showed that the presence of heat flow produces no additional singularities. In other words, at the crack tip, the singularities of the thermal stress and mechanical stresses are identical, i.e. $1/\sqrt{r}$.

In the past decades many researchers have studied a weakened infinite or semi-infinite plane being generally under uniform heat flow. For instance, the thermal stress singularities at the tips of an arbitrarily oriented crack in a semi-infinite medium under uniform heat flow have been analyzed by Sekine [3]. In this work, the problem of a half-plane weakened by insulated crack under uniform heat flow was investigated and the stress intensity factors for modes I and II were obtained. Atkinson and Clements [4]solved two-dimensional Griffith crack obstructing a uniform heat flux in a general anisotropic medium by the techniques of Fourier transforms and multiple integrations. Sturla and Barber [5, 6]considered the same problem in a general anisotropic infinite plane by using a Green's function and gave the exact solutions of the mixed-mode thermal stress intensity factors

In some cases, the mediums were made of nonhomogeneous materials exposed to thermal loading, which necessitated a thermomechanical analysis. As an illustration, a crack in a strip of functionally graded material was investigated by Noda and Jin[7] and thermal stress intensity factors were obtained. Also, the analysis of a semi-infinite nonhomogeneous thermoelastic solid containing a crack subjected to steady heat flux over the boundary was investigated by Jin and Noda [8]. The problem of an edge crack in a semi-infinite nonhomogeneous plate under steady state heat flux was also studied by Jin and Noda [9]. The problem of a functionally graded layer weakened by an embedded or surface crack perpendicular to its boundaries is investigated by Erdogan and Wu [10]. Thermomechanical properties are assumed to be continuous and the elastic layer is under statically self-equilibrating thermal or residual stresses. Borgi et al. [11]investigated the problem of an infinite functionally graded medium with a partially insulated crack subjected to a steady-state heat flux applied away from the crack region as well as mechanical stresses applied as crack surface tractions.

Coatings also play crucial role in the design of structures subjected to severe thermal conditions. The plane strain thermal stress problem for an interface crack in a homogenous substrate with a graded coating was studied by Lee and Erdogan [12]. Itou [13] solved the thermal stress problem of an interfacial layer bonded between two dissimilar elastic half planes weakened by a crack. The thermal fracture problem of a functionally graded coating-substrate structure of finite thickness with a partially insulated interface crack is investigated by Zhou and Lee [14]. Choi [15] examined the steady-state thermoelastic problem of a crack at an arbitrary angle to the graded interfacial zone in bonded media. In practice, structures are usually weakened by multiple cracks which, in close distances, demonstrate considerable interaction. The analysis of a periodic array of embedded and edge cracks in an infinite elastic strip are investigated by Rizk [16, 17].

In this study, the cracked surface was heated and compressive stresses occurred near the heated surface causing the crack surfaces to come into contact along a certain contact length. Later, the problem of two periodic edge cracks in an elastic infinite strip under thermal loading was also studied by Rizk and Fattah [18].

In the case of dynamic thermal loading and thermal shock, a transient thermomechanical analysis should be performed. Nied [19]investigated the transient thermal stress problem for an elastic strip weakened by an edge crack which was insulated on one face and cooled by surface convection on the face containing the edge crack.

Rizk et al.[20]studied the transient thermal stress in a strip with an edge crack. In another paper, Rizk et al. [21]investigated the effects of a sudden thermal transient stresses for plate of finite thickness containing an edge crack. In this study, the stress intensity factors for various crack sizes and cooling rates have been investigated. The transient thermal stresses around a crack in a semi-infinite thermoelastic body under a thermal impact using the hyperbolic conduction was determined by Chen and Hu[22]. Hu and Chen [23]also investigated the transient temperature and thermal stresses around a crack in a thermoelastic strip under a temperature impact loading. Among different methods for the analysis of cracks, the distributed dislocation technique has considerable advantages. Analysis of multiple cracks as well as providing full field closed form solutions are feasible using this technique. However, all the aforementioned investigations lack this advantageous technique. The study of an insulated crack in an anisotropic half-plane under a uniform heat flux using distributed dislocation technique was analyzed by Liu and Kardomates [24].Ravandi and Fariborz [25] studied the cracked layer fixed at a boundary and free of traction at the other boundary with specified temperature at the boundary using the distributed dislocation technique.

As can be seen, there are only a few investigations in the last decade employed this technique to solve the problem. This method, not only, provides a closed form solutions to the crack problems, but also, is capable of analyzing multiple arbitrary cracks in a medium. Besides, the majority of the problems were restricted to solve the problems being under a uniform heat flow. Therefore, the aim of this study is to present a closed-form solution for a half-plane with multiple cracks which is subjected to the point load thermal and mechanical loadings. The novelty of the current investigation lies in the introduction of a Volterra type thermoelastic dislocation, applying the thermo-mechanical point loads on the boundary, and presenting a Green solution with the help of distributed dislocation technique which is capable to determine the stress intensity factors for various crack configuration.

In section 2, at first, a Volterra type thermoelastic dislocation is introduced in the half-plane and the temperature distribution and stress fields are derived. Then, the stress and thermal fields of a defect-less half-plane under external mechanical and thermal loadings are determined. These subsections provide the required elements of the distributed dislocation technique. In section 3, the distributed dislocation technique is utilized to model the half-plane weakened by multiple cracks leading to a set of integral equations. In this study, only the case of the complete opening of cracks is considered. The integral equations are numerically solved and the stress intensity factors (SIFs) are determined. Several examples are presented including half-plane with cracks of different geometries and the effect of the loading conditions on SIFs are investigated.

2 Fundamentals

We intend to employ the distributed dislocation technique for the thermoelastic analysis of a half-plane weakened by multiple cracks. For this purpose, it is required to study the problem of a dislocation in the half-plane. Moreover, we shall determine the behavior of the uncracked half-plane subjected to external thermal and mechanical loadings. These tasks are carried out in this section.

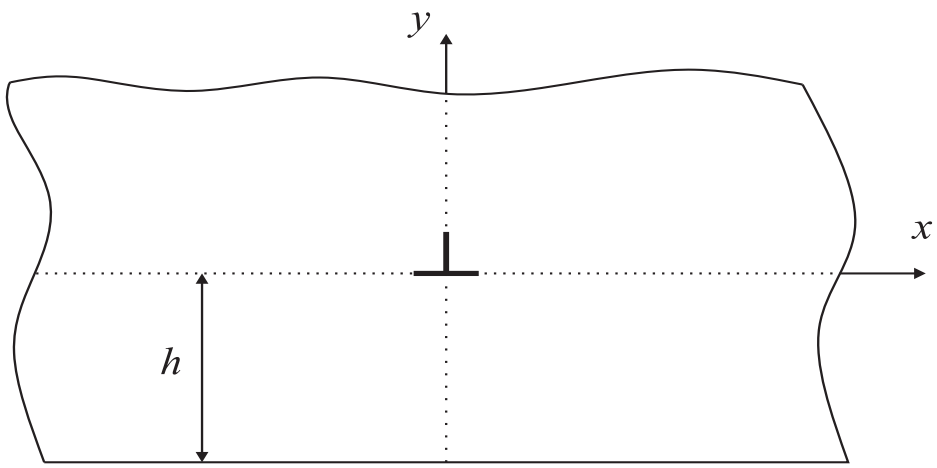

Figure 1 Half-plane weakened by a thermoelastic dislocation.

2.1 Thermoelastic analysis of a half-plane weakened by a dislocation

Let us consider an elastic half-plane containing a thermoelastic dislocation located at origin of coordinates as depicted in Figure (1). The dislocation line is considered to be in the positive direction of the *z*-axis. Here, the effects of inertia and thermoelastic coupling are neglected which leads to an uncoupled and quasi-static problem of thermoelasticity. By the use of Fourier's heat conduction equation, governing equation for temperature field in Cartesian coordinates and constant properties reads [26]

$$\nabla^2 T(x,y) = \frac{\partial^2 T}{\partial x^2} + \frac{\partial^2 T}{\partial y^2} = 0 \tag{1}$$

Where $T(x,y)$ is temperature field and ∇^2 is the Laplacian operator. The heat equation (1) should satisfy the following conditions

$$\begin{aligned} &T(x,0^+) - T(x,0^-) = \delta_T H(x), \\ &Q_y(x,0^+) = Q_y(x,0^-), \\ &T(x,-h) = 0. \end{aligned} \tag{2}$$

In Eq. (2), $H(..)$ is the Heaviside step-function, Q_y is the heat flux in the *y*-direction, and δ_T is the temperature discontinuity along the dislocation cut.

It should be mentioned that a crack with insulated faces perturbs a heat flux. Since a crack can be represented as a dislocation array, it is reasonable to assume that the heat flux perturbs across the dislocation cut. According to the second condition in Eqs. (2), the continuity of the heat flux along the dislocation cut requires that

$$\frac{\partial T(x,0^+)}{\partial y} = \frac{\partial T(x,0^-)}{\partial y} \tag{3}$$

This boundary value problem is solved by applying the complex Fourier transformation to Eq. (1). Then, the solution to the temperature field reads

$$T(x,y)=\frac{\delta_T}{2\pi}\int_{-\infty}^{+\infty}\frac{|\zeta|(\pi\delta(\zeta)-\frac{i}{\zeta})}{[(|\zeta|-\zeta)e^{-2\zeta h}-(|\zeta|+\zeta)]}(e^{\zeta y}-e^{-\zeta(2h+y)})e^{i\zeta x}d\zeta, \qquad -h\le y\le 0$$

$$T(x,y)=\frac{\delta_T}{2\pi}\int_{-\infty}^{+\infty}-\frac{\zeta(\pi\delta(\zeta)-\frac{i}{\zeta})(1+e^{-2\zeta h})}{[(|\zeta|-\zeta)e^{-2\zeta h}-(|\zeta|+\zeta)]}e^{-|\zeta|y}e^{i\zeta x}d\zeta \qquad y\ge 0 \qquad (4)$$

Where $\delta(..)$ is the Dirac delta function.

In a homogenous isotropic medium, the heat flux Q_n along the unit vector $\bar{n}=n_x\hat{i}+n_y\hat{j}$ is given by [26]

$$Q_n^T=-K\bar{\nabla}T.\bar{n} \qquad (5)$$

Where K is the thermal conductivity. Once the temperature field from Eq. (4) is substituted in Eq. (5), the heat flux is obtained as

$$Q_n^T(x,y)=\frac{K\delta_T}{2\pi}[-n_x(\frac{y}{x^2+y^2}+\frac{2h+y}{x^2+(2h+y)^2})+n_y(\frac{x}{x^2+y^2}+\frac{x}{x^2+(2h+y)^2})] \qquad (6)$$

It is observed that the heat flux $Q_n^T(x,y)$ is Cauchy singular at the dislocation core, i.e. $Q_n\approx 1/r$, as $r=\sqrt{x^2+y^2}\to 0$.

In order to determine the stress field, we can make use of the basic equations including compatibility equation and the constitutive law given by[26]

$$\frac{\partial^2\varepsilon_x}{\partial y^2}+\frac{\partial^2\varepsilon_y}{\partial x^2}=2\frac{\partial^2\varepsilon_{xy}}{\partial x\partial y},$$

$$\varepsilon_x=\frac{1}{E}(\sigma_x-\nu\sigma_y)+\alpha T, \qquad (7)$$

$$\varepsilon_y=\frac{1}{E}(\sigma_y-\nu\sigma_x)+\alpha T$$

The stress components in terms of Airy stress function $\varphi(x,y)$ may be expressed as

$$\sigma_{xx}=\frac{\partial^2\varphi(x,y)}{\partial y^2}, \qquad \sigma_{yy}=\frac{\partial^2\varphi(x,y)}{\partial x^2}, \qquad \sigma_{xy}=-\frac{\partial^2\varphi(x,y)}{\partial x\partial y} \qquad (8)$$

The substitution of Eq. (8) into the compatibility equation and considering the constitutive law in uncoupled theory of thermoelasticity, we arrive at the following differential equation

$$\nabla^2(\nabla^2\varphi+\frac{8\mu\alpha}{\kappa+1}T)=0 \qquad (9)$$

Where $\kappa=3-4\nu$ and $\alpha=\alpha_T/(1+\nu)$ for the plane strain, and $\kappa=(3-\nu)/(1+\nu)$ and $\alpha=\alpha_T$ for generalized plane stress. Substituting the stress components (8) into the constitutive law, the strain components read

$$\varepsilon_x=\frac{\partial u}{\partial x}=\frac{1}{8\mu}[(\kappa+1)\frac{\partial^2\varphi}{\partial y^2}-(3-\kappa)\frac{\partial^2\varphi}{\partial x^2}]+\alpha T,$$

$$\varepsilon_y=\frac{\partial v}{\partial y}=\frac{1}{8\mu}[(\kappa+1)\frac{\partial^2\varphi}{\partial x^2}-(3-\kappa)\frac{\partial^2\varphi}{\partial y^2}]+\alpha T,$$

$$\gamma_{xy}=\frac{\partial u}{\partial y}+\frac{\partial v}{\partial x}=-\frac{1}{\mu}\frac{\partial^2\phi}{\partial x\partial y} \qquad (10)$$

While (u,v) are the displacement fields of the half-plane. The boundary value problem for the elastic half-plane with thermoelastic dislocations includes the conditions

$$\begin{aligned}
&\sigma_{yy}(x,-h)=0\ ,\\
&\sigma_{xy}(x,-h)=0,\\
&\sigma_{yy}(x,0^+)=\sigma_{yy}(x,0^-),\\
&\sigma_{xy}(x,0^+)=\sigma_{xy}(x,0^-),\\
&u(x,0^+)-u(x,0^-)=b_x H(x),\\
&v(x,0^+)-v(x,0^-)=b_y H(x)
\end{aligned} \tag{11}$$

Where b_x and b_y are the Burgers vectors for the glide and climb edge dislocations, respectively. The general solution of the differential equation (9) is

$$\varphi=\varphi^p+\varphi^h \tag{12}$$

Where φ^p and φ^h are particular and homogenous solutions, respectively, and should satisfy the following relations

$$\begin{aligned}
&\nabla^2\varphi^p+\frac{8\mu\alpha}{\kappa+1}T=0,\\
&\nabla^4\varphi^h=0
\end{aligned} \tag{13}$$

Employing the complex Fourier transform together with the assumption $\lim_{|x|\to\infty}[\varphi^p,\varphi^h]\to 0$, the Eqs (13) are rewritten as

$$\begin{aligned}
&(\frac{d^2}{dy^2}-\zeta^2)\varphi^{*p}+\frac{8\mu\alpha}{\kappa+1}T^*(\zeta,y)=0,\\
&(\frac{d^2}{dy^2}-\zeta^2)^2\varphi^{*h}=0
\end{aligned} \tag{14}$$

Moreover, considering Eqs. (8) and (10), Fourier transformation of conditions (11) reaches

$$\begin{aligned}
&\varphi^*(\zeta,-h)=0\ ,\quad \frac{d}{dy}\varphi^*(\zeta,-h)=0,\\
&\varphi^*(\zeta,0^+)=\varphi^*(\zeta,0^-)\ ,\quad \frac{d}{dy}\varphi^*(\zeta,0^+)=\frac{d}{dy}\varphi^*(\zeta,0^-),\\
&\frac{-i}{8\mu\zeta}\{(1+\kappa)[\frac{\partial^2\phi^*(\zeta,0^+)}{\partial y^2}-\frac{\partial^2\phi^*(\zeta,0^-)}{\partial y^2}]-(\kappa-3)\zeta^2[\phi^*(\zeta,0^+)-\phi^*(\zeta,0^-)]\}\\
&+\frac{i\alpha}{\zeta}\left(T^*(\zeta,0^+)-T^*(\zeta,0^-)\right)=b_x(\pi\delta(\zeta)-\frac{i}{\zeta}),\\
&\frac{1}{8\mu}\{\frac{(1+\kappa)}{\zeta^2}[\frac{\partial^3\phi^*(\zeta,0^+)}{\partial y^3}-\frac{\partial^3\phi^*(\zeta,0^-)}{\partial y^3}]-(\kappa+5)[\frac{\partial\phi^*(\zeta,0^+)}{\partial y}-\frac{\partial\phi^*(\zeta,0^-)}{\partial y}]\}\\
&+\frac{\alpha}{\zeta^2}(\frac{\partial T^*(\zeta,0^+)}{\partial y}-\frac{\partial T^*(\zeta,0^-)}{\partial y})=b_y(\pi\delta(\zeta)-\frac{i}{\zeta})
\end{aligned} \tag{15}$$

The differential equations (14) are solved considering the conditions (15). Then by employing the Fourier inversion, the Airy stress function reads

$$\varphi(x,y)=\frac{1}{\pi}\int_0^{\infty}\{i(\alpha L_T\,\delta_T+b_y\,L_y)\sin(\xi x)+b_x\,L_x\cos(\xi x)\}d\xi \tag{16}$$

Where L_T, L_Y and L_X are

$$L_T=\frac{2ie^{-(2h+y)\xi}\mu(-y+e^{2(h+y)\xi}y+2h^2\xi+2hy\xi)}{(1+k)\xi^2}$$

$$L_X=-\frac{2e^{-(2h+y)\xi}\mu(-y+e^{2(h+y)\xi}y+2h^2\xi+2hy\xi)}{(1+k)\xi}$$

$$L_Y=\frac{2ie^{-(2h+y)\xi}\mu(1-e^{2(h+y)\xi}+2h\xi+y\xi+e^{2(h+y)\xi}y\xi+2h^2\xi^2+2hy\xi^2)}{(1+k)\xi^2} \tag{17}$$

By substituting the Airy function (16) into (8), the stress components read

$$\sigma_{xx}(x,y)=\frac{1}{\pi}\int_0^{\infty}D^2\{i(\alpha L_T\,\delta_T+b_y\,L_y)\sin(\xi x)+b_x\,L_x\cos(\xi x)\}d\xi$$

$$\sigma_{yy}(x,y)=\frac{1}{\pi}\int_0^{\infty}\zeta^2\{i(\alpha L_T\,\delta_T+b_y\,L_y)\sin(\xi x)-b_x\,L_x\cos(\xi x)\}d\xi$$

$$\sigma_{xy}(x,y)=\frac{-1}{\pi}\int_0^{\infty}D\xi\{i(\alpha L_T\,\delta_T+b_y\,L_y)\cos(\xi x)-b_x\,L_x\sin(\xi x)\}d\xi \tag{18}$$

Here, $D\equiv\partial/\partial y$ is the differential operator. Employing the integral expressions given in [27], the stress field (18) is simplified to

$$\begin{Bmatrix}\sigma_{xx}\\ \sigma_{yy}\\ \sigma_{xy}\end{Bmatrix}=\frac{2\mu}{\pi(1+\kappa)}\left\{\frac{1}{(x^2+y^2)^2}\left[\alpha\delta_T\begin{Bmatrix}Q_x+xy(x^2+y^2)\\ -xy(x^2+y^2)\\ Q_{xy}+y^2(x^2+y^2)\end{Bmatrix}+b_x\begin{Bmatrix}y(3x^2+y^2)\\ y(y^2-x^2)\\ x(y^2-x^2)\end{Bmatrix}-b_y\begin{Bmatrix}x(x^2-y^2)\\ x(3y^2+x^2)\\ y(x^2-y^2)\end{Bmatrix}\right]\right.$$
$$\left.+\frac{1}{(x^2+(y+2h)^2)^3}\left[\alpha\delta_T\begin{Bmatrix}P_x\\ P_y\\ P_{xy}\end{Bmatrix}+b_x\begin{Bmatrix}M_x\\ M_y\\ M_{xy}\end{Bmatrix}+b_y\begin{Bmatrix}N_x\\ N_y\\ N_{xy}\end{Bmatrix}\right]\right\} \tag{19}$$

In the equations (19), Q_x and Q_{xy} are defined as

$$Q_x=2(x^2+y^2)^2\int_0^{\infty}\frac{e^{\xi y}}{\xi}\sin(\xi x)d\xi$$

$$Q_{xy}=-(x^2+y^2)^2\int_0^{\infty}\frac{e^{\xi y}}{\xi}\cos(\xi x)d\xi \tag{20}$$

and functions $P_{...}, M_{...}$ and $N_{...}$ are given in the Appendix. It is noted that the stress components (19) exhibit the familiar Cauchy type singularity at the dislocation core. The dislocation solution in half-plane, cited for instance in [28], may readily be recovered by letting $\delta_T = 0$ in Eq. (19).

2.2 Thermoelastic Analysis of a defect-less half-plane under external load

In order to employ the distributed dislocation technique, we need to know the behavior of a half-plane (in the absence of defects) subjected to external thermal and mechanical loads. The theory of linear thermoelasticity is based on linear addition of thermal strains to mechanical strains. First, we assume that the temperature on the boundary of the half-plane is $T(x,-h) = T_0 e^{-\gamma|x|}$, satisfying $\lim_{|x|\to\infty}[T(x,-h)] \to 0$. Hence, the thermal conditions may be expressed as

$$T(x,-h) = T_0 e^{-\gamma|x|} \tag{21}$$

Following a similar procedure as we followed in the previous section, it can be shown that the solution of Eq. (1) together with conditions (21) reads

$$T(x,y) = \frac{2T_0\gamma}{\pi}\int_0^\infty \frac{e^{-\xi(h+y)}}{(\gamma^2+\xi^2)}\cos(\xi x)d\xi \tag{22}$$

The heat flux Q_n^T due to above temperature distribution is

$$Q^T{}_n(x,y) = \frac{2KT_0\gamma}{\pi}[n_x\int_0^\infty \frac{\xi e^{-\xi(h+y)}}{(\gamma^2+\xi^2)}\sin(\xi x)d\xi + n_y\int_0^\infty \frac{\xi e^{-\xi(h+y)}}{(\gamma^2+\xi^2)}\cos(\xi x)d\xi] \tag{23}$$

Next, we consider a half-plane which is subjected to an in-plane mechanical point force with magnitude σ_0 and τ_0 at coordinates $(0,-h)$ on the boundary. Consequently, the boundary conditions read

$$\sigma_{yy}(x,-h) = \sigma_0\delta(x)\ ,\sigma_{xy}(x,-h) = \tau_0\delta(x) \tag{24}$$

Following a similar procedure as outlined in the previous section for the dislocation solution, the stress field due this external mechanical loading can be derived.
Finally, the stress field due to the above-mentioned in-plane mechanical and thermal loadings reads

$$\begin{aligned}
\sigma_{xx}(x,y) &= \frac{2x^2(\sigma_0(y+h)-\tau_0 x)}{\pi(x^2+(h+y)^2)^2} + \frac{4\mu\alpha T_0\gamma}{\pi(1+\kappa)}\int_0^\infty \frac{(y\xi-2)e^{-\xi(h+y)}}{(\gamma^2+\xi^2)}\cos(\xi x)d\xi \\
\sigma_{yy}(x,y) &= \frac{2(h+y)^2(\sigma_0(y+h)-\tau_0 x)}{\pi(x^2+(h+y)^2)^2} - \frac{4y\mu\alpha T_0\gamma}{\pi(1+\kappa)}\int_0^\infty \frac{\xi e^{-\xi(h+y)}}{(\gamma^2+\xi^2)}\cos(\xi x)d\xi \\
\sigma_{xy}(x,y) &= \frac{2x(y+h)(\sigma_0(y+h)-\tau_0 x)}{\pi(x^2+(h+y)^2)^2} - \frac{4\mu\alpha T_0\gamma}{\pi(1+\kappa)}\int_0^\infty \frac{(y\xi-1)e^{-\xi(h+y)}}{(\gamma^2+\xi^2)}\sin(\xi x)d\xi
\end{aligned} \tag{25}$$

In the following section, the dislocation solution together with the solution to the defect-less half-plane are employed to construct the integral equations representing the crack.

3 Thermoelastic analysis of half-plane with multiple cracks

The thermoelastic dislocation solutions accomplished in the previous section may be used to analyze a half-plane with several arbitrarily oriented cracks subjected to the thermomechanical loading. The stress and heat flux components caused by the climb, glide, and thermal

dislocations located at (x_0, y_0) can be obtained by replacing (x_0, y_0) with $(x-x_0, y-y_0)$ in Eqs. (6) and (19). Consequently the stress and heat flux components read

$$\begin{aligned} \sigma_{ij}(x,y) &= k_{ij}^{t}(x,y)\delta_T + k_{ij}^{x}(x,y)b_x + k_{ij}^{y}(x,y)b_y \\ Q_i(x,y) &= q_i(x-x_0,y)\delta_T, \quad \{i,j\} \in \{x,y\} \end{aligned} \tag{26}$$

where k_{ij}^{m}, $m \in \{\mathrm{t}, x, y\}$ are the coefficients of δ_T, b_x and b_y and may be deduced from Eq. (19).

Let N be the number of cracks in the half-plane. A crack configuration with respect to the Cartesian coordinate $x-y$ may be described in parametric form as:

$$\begin{aligned} x_i &= \alpha_i(\eta) \\ y_i &= \beta_i(\eta) \qquad -1 \le \eta \le 1, \;\; i \in \{1,2,...,N\} \end{aligned} \tag{27}$$

The moveable orthogonal coordinate systems (s,n) are chosen on the *i*th crack such that the origins locate on the cracks while the *s*-axes remain tangent to the cracks surfaces. The stress components and heat flux may be transformed to (s,n) coordinates as

$$\begin{aligned} \sigma_n &= \frac{\sigma_{xx}+\sigma_{yy}}{2} - \frac{\sigma_{xx}-\sigma_{yy}}{2}\cos(2\theta_i) - \sigma_{xy}\sin(2\theta_i), \\ \sigma_s &= -\frac{\sigma_{xx}-\sigma_{yy}}{2}\sin(2\theta_i) + \sigma_{xy}\cos(2\theta_i), \\ Q_n &= Q_y\cos(\theta_i) - Q_x\sin(\theta_i) \end{aligned} \tag{28}$$

The components of Burgers vectors b_x and b_y are transformed to the (s,n) coordinate on the surface of *j*th crack. The relationships between components of Burgers vectors in two coordinate systems are

$$\begin{aligned} b_x &= b_s\cos(\theta_j) - b_n\sin(\theta_j), \\ b_y &= b_s\sin(\theta_j) + b_n\cos(\theta_j) \end{aligned} \tag{29}$$

where $\theta_k = \tan^{-1}(\beta_k'(t)/\alpha_k'(t)), \quad k \in \{i,j\}$ is the angle between *s*- and *x*-axes.

Cracks can be modeled as a distribution of thermoelastic dislocations with the densities $B_{mj}(\mathrm{t}), \quad m \in \{T,s,n\}$ as well. The components of tractions vector and heat flux along the cracks surfaces due to the dislocation distribution are

$$\begin{aligned} \sigma_{ni}(x(\eta),y(\eta)) &= \sum_{j=1}^{N}\int_{-1}^{1}\{K_{11ij}(\eta,t)B_{Tj}(t) + K_{12ij}(\eta,t)B_{sj}(t) + K_{13ij}(\eta,t)B_{nj}(t)\}\sqrt{[\alpha_j'(t)]^2+[\beta_j'(t)]^2}\,dt, \\ \sigma_{si}(x(\eta),y(\eta)) &= \sum_{j=1}^{N}\int_{-1}^{1}\{K_{21ij}(\eta,t)B_{Tj}(t) + K_{22ij}(\eta,t)B_{sj}(t) + K_{23ij}(\eta,t)B_{nj}(t)\}\sqrt{[\alpha_j'(t)]^2+[\beta_j'(t)]^2}\,dt, \\ Q_{ni}(x(\eta),y(\eta)) &= \sum_{j=1}^{N}\int_{-1}^{1}K^{t}(\eta,t)B_{Tj}(t)\sqrt{[\alpha_j'(t)]^2+[\beta_j'(t)]^2}\,dt \qquad i \in \{1,2,...,N\}, \quad -1 \le \eta \le 1 \end{aligned} \tag{30}$$

Where the kernels in Eq. (30) are given by

$$K_{11ij}(\eta,\mathrm{t}) = -\frac{1}{2}\left(k_{xx}^{1} - k_{yy}^{1}\right)\cos(2\theta_i) - k_{xy}^{1}\sin(2\theta_i) + \frac{1}{2}\left(k_{xx}^{1} + k_{yy}^{1}\right),$$

$$K_{12ij}(\eta,\mathrm{t}) = \frac{1}{2}\left[\left(k_{yy}^{2} - k_{xx}^{2}\right)\cos(\theta_j) + \left(k_{yy}^{3} - k_{xx}^{3}\right)\sin(\theta_j)\right]\cos(2\theta_i)$$
$$-\left[k_{xy}^{2}\cos(\theta_j) + k_{xy}^{3}\sin(\theta_j)\right]\sin(2\theta_i) + \frac{1}{2}\left(k_{xx}^{2} + k_{yy}^{2}\right)\cos(\theta_j) + \frac{1}{2}\left(k_{xx}^{3} + k_{yy}^{3}\right)\sin(\theta_j),$$

$$K_{13ij}(\eta,\mathrm{t}) = \frac{1}{2}\left[\left(k_{yy}^{3} - k_{xx}^{3}\right)\cos(\theta_j) + \left(k_{xx}^{2} - k_{yy}^{2}\right)\sin(\theta_j)\right]\cos(2\theta_i)$$
$$-\left[k_{xy}^{3}\cos(\theta_j) - k_{xy}^{2}\sin(\theta_j)\right]\sin(2\theta_i) + \frac{1}{2}\left(k_{xx}^{3} + k_{yy}^{3}\right)\cos(\theta_j) - \frac{1}{2}\left(k_{xx}^{3} + k_{yy}^{3}\right)\sin(\theta_j),$$

$$K_{21ij}(\eta,\mathrm{t}) = -\frac{1}{2}\left(k_{xx}^{1} - k_{yy}^{1}\right)\sin(2\theta_i) + k_{xy}^{1}\cos(2\theta_i),$$

$$K_{22ij}(\eta,\mathrm{t}) = -\frac{1}{2}\left[\left(k_{xx}^{2} - k_{yy}^{2}\right)\cos(\theta_j) + \left(k_{xx}^{3} - k_{yy}^{3}\right)\sin(\theta_j)\right]\sin(2\theta_i)$$
$$+\left[k_{xy}^{2}\cos(\theta_j) + k_{xy}^{3}\sin(\theta_j)\right]\cos(2\theta_i),$$

$$K_{23ij}(\eta,\mathrm{t}) = -\frac{1}{2}\left[\left(k_{xx}^{3} - k_{yy}^{3}\right)\cos(\theta_j) + \left(k_{yy}^{2} - k_{xx}^{2}\right)\sin(\theta_j)\right]\sin(2\theta_i)$$
$$+\left[k_{xy}^{3}\cos(\theta_j) - k_{xy}^{2}\sin(\theta_j)\right]\cos(2\theta_i),$$

$$K^{t} = q_y\cos(\theta_i) - q_x\sin(\theta_i) \tag{31}$$

In this analysis, it is assumed that the problem is linear. So, the solution of the crack problem is considered to be the sum of two sub-problems. The first problem is the thermoelastic analysis of a half-plane in the absence of cracks under external thermomechanical loadings which yields the traction and heat flux with opposite signs for a perfect conduction crack. The second problem gives the corrective solution which is generated by continuously distributing the dislocations along the crack faces. Accordingly, to satisfy the traction free condition of the crack faces, the left-hand sides of Eq. (30) are the traction and heat flux with opposite sign obtained from thermoelasticity problem of a half-plane under external thermomechanical loadings.

Employing the definition of the dislocation density function, the equations for crack opening displacement and temperature discontinuity across the *i*th crack become

$$u_{ni}^{+}(\eta) - u_{ni}^{-}(\eta) = \int_{-1}^{\eta}\left[\cos\left(\theta_i(\eta) - \theta_i(t)\right)B_{ni}(t) - \sin\left(\theta_i(\eta) - \theta_i(t)\right)B_{si}(t)\right]\sqrt{[\alpha_i'(t)]^2 + [\beta_i'(t)]^2}\,dt,$$

$$u_{si}^{+}(\eta) - u_{si}^{-}(\eta) = \int_{-1}^{\eta}\left[\cos\left(\theta_i(\eta) - \theta_i(t)\right)B_{si}(t) + \sin\left(\theta_i(\eta) - \theta_i(t)\right)B_{ni}(t)\right]\sqrt{[\alpha_i'(t)]^2 + [\beta_i'(t)]^2}\,dt,$$

$$T_i^{+}(\eta) - T_i^{-}(\eta) = \int_{-1}^{\eta} B_{Ti}(t)\sqrt{[\alpha_i'(t)]^2 + [\beta_i'(t)]^2}\,dt \qquad -1 \le \eta \le 1,\ i \in \{1,2,...,N\} \tag{32}$$

Where u_n, u_s, and T are displacement components in the normal and tangential directions and temperature, respectively. For cracks embedded in the half-plane Eq. (30) should be complimented with the following closure requirements:

$$\int_{-1}^{1}[\cos(\theta_i(1)-\theta_i(t))B_{ni}(t)-\sin(\theta_i(1)-\theta_i(t))B_{si}(t)]\sqrt{[\alpha_i'(t)]^2+[\beta_i'(t)]^2}\,dt=0,$$

$$\int_{-1}^{1}[\cos(\theta_i(1)-\theta_i(t))B_{si}(t)+\sin(\theta_i(1)-\theta_i(t))B_{ni}(t)]\sqrt{[\alpha_i'(t)]^2+[\beta_i'(t)]^2}\,dt=0,$$

$$\int_{-1}^{1}B_{Ti}(t)\sqrt{[\alpha_i'(t)]^2+[\beta_i'(t)]^2}\,dt=0 \qquad i\in\{1,2,...,N\} \tag{33}$$

In studying the fracture of structural components due to the thermal stresses, it is important to consider the thermal stress singularities at the tips of crack[2, 3]

The singularity of heat flux, in the vicinity of a crack tip, is the same as that of stress fields. Therefore, the dislocation densities for an embedded crack are given by

$$B_{li}(\mathrm{t})=\frac{g_{li}(t)}{\sqrt{1-t^2}} \quad -1\le t\le 1,\quad l\in\{x,y,T\},\quad i\in\{1,2,...,N\} \tag{34}$$

Referring to the definitions of modes I and II stress intensity factors for embedded cracks given by Fotuhi and Fariborz [29], the intensity factors lead to

$$\begin{Bmatrix}K_{IL}\\K_{IIL}\end{Bmatrix}=-\frac{2\mu}{1+\kappa}\left([\alpha_i'(-1)]^2+[\beta_i'(-1)]^2\right)^{\frac{1}{4}}\begin{Bmatrix}g_{ni}(-1)\\g_{si}(-1)\end{Bmatrix},$$

$$\begin{Bmatrix}K_{IR}\\K_{IIR}\end{Bmatrix}=\frac{2\mu}{1+\kappa}\left([\alpha_i'(1)]^2+[\beta_i'(1)]^2\right)^{\frac{1}{4}}\begin{Bmatrix}g_{ni}(1)\\g_{si}(1)\end{Bmatrix} \tag{35}$$

where the subscripts L and R designate the left and right crack tips respectively. Eq. (34) are substituted into Eqs. (30) and (33), and the resultant equations are solved via the technique developed by Erdogan et al. [30] to determine $g_{li}(t)$ in which $i\in\{1,2,...,N\}$.The values of $g_{li}(\mp 1)$ should be substituted into Eq. (35) to obtain SIFs.

4 Results and discussions

In this section the results of some examples for a half-plane weakened by arbitrary number of parallel, collinear and oblique cracks under diverse loading conditions including mechanical, thermal and thermo-mechanical loadings are presented. In all the following examples, the thermoelastic and material constants are $k=51.9(W/m.K)$, $\alpha_T=2.53\times10^{-5}\,(^{\circ}C^{-1})$ and $\nu=0.29$. Moreover, we are only concerned with the full opening of cracks. Note that, the temperature distribution on the boundary of the half-plane was taken as $T(x,-h)=T_0e^{-\gamma|x|}$, where $T_0=100\,^{\circ}C$ and γ is taken to be 5 and $10(1/m)$.To render the results dimensionless, unless otherwise stated, stress intensity factors for straight cracks was normalized by $K_0=\sigma_0/\sqrt{a}$.

Table (1) depicts the SIFs of an isotropic half-plane subjected to mechanical loadings which is shown in Figure 2. The results have a great agreement with those reported by Ashbaugh [31].

4.1 Medium under in-plane mechanical loadings

Figures (3a) and (3b) show the effects of crack orientation on the mode I SIFs. In this case, the half-plane is subjected to normal and shear point loads. It can be seen that the stress intensity factors are varying with respect to the angle of rotation. It is evident that the mode I SIF increase dramatically and hits its peak around 60 degree. Obviously, at $\theta=\pi/2$, the traction on the crack surface vanishes and the stress intensity factors are zero.

Table1 Straight crack in an isotropic half-plane for right and left crack tips

$\sigma_0 = 1$		h				
$\tau_0 = 0$		∞	4.0	1.0	0.4	0.1
Ashbaugh[31]	K_I/K_0	1	1.045	1.511	2.905	14.01
		1	1.045	1.511	2.905	14.01
	K_{II}/K_0	0	0.0055	0.1849	0.9940	8.812
		0	-0.0055	-0.1849	-0.9940	-8.812
Present study	K_I/K_0	1	1.0451	1.5110	2.9056	14.01
		1	1.0451	1.5510	2.9056	14.01
	K_{II}/K_0	0	0.0055	0.1849	0.9940	8.8133
		0	-0.0055	-0.1849	-0.9940	-8.8133
$\sigma_0 = 0$		h				
$\tau_0 = 1$		∞	4.0	1.0	0.4	0.1
Ashbaugh[31]	K_I/K_0	0	-0.0053	-0.1331	-0.3876	-0.8709
		0	0.0053	0.1331	0.3876	0.8709
	K_{II}/K_0	1	1.014	1.087	1.133	1.384
		1	1.014	1.087	1.133	1.384
Present	K_I/K_0	0	-0.0053	-0.1331	-0.3876	-0.8710
		0	0.0053	0.1331	0.3876	0.8710
	K_{II}/K_0	1	1.0141	1.0873	1.1329	1.3842
		1	1.0141	1.0873	1.1329	1.3842

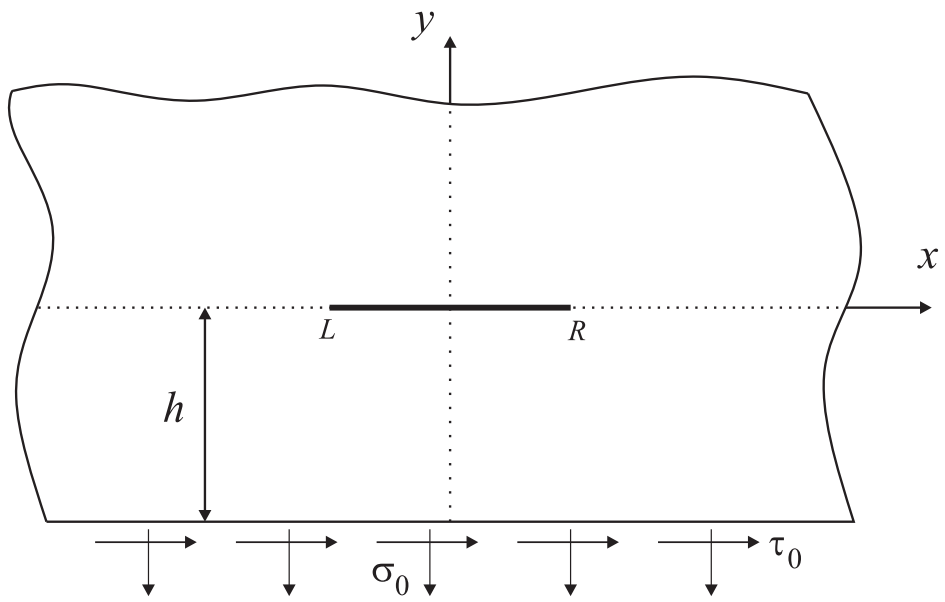

Figure 2 A weakened half-plane under uniform mechanical loading.

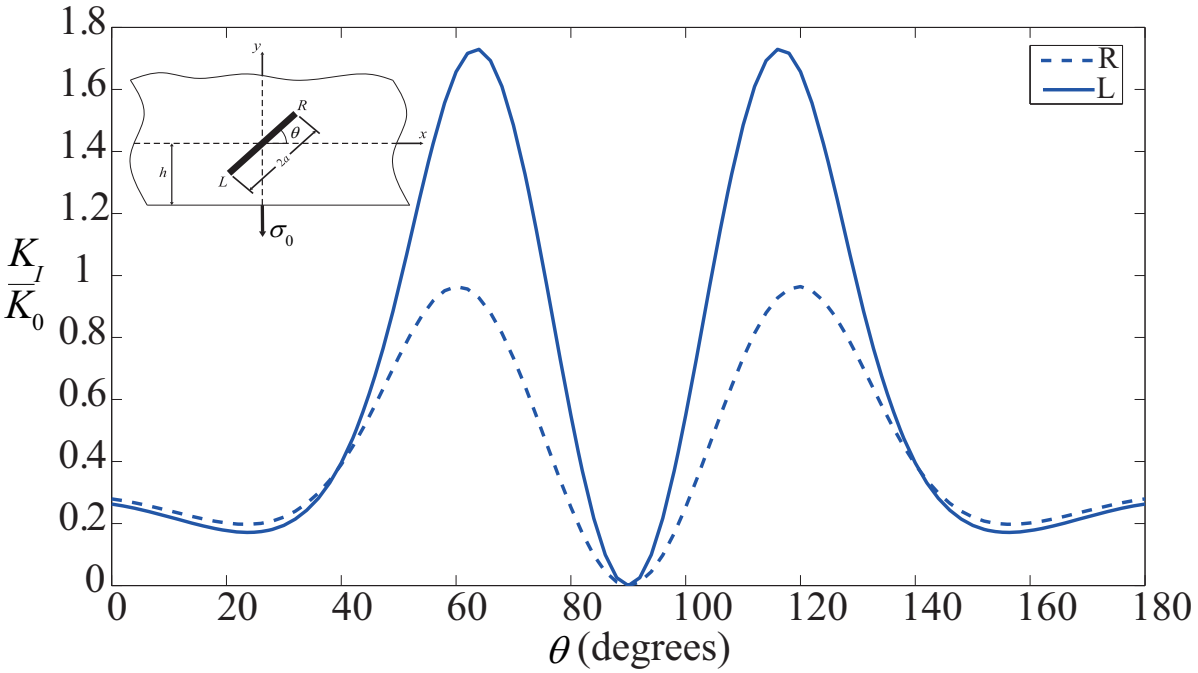

Figure 3a Non-dimensional mode I stress intensity factors for an oblique crack under normal point load.

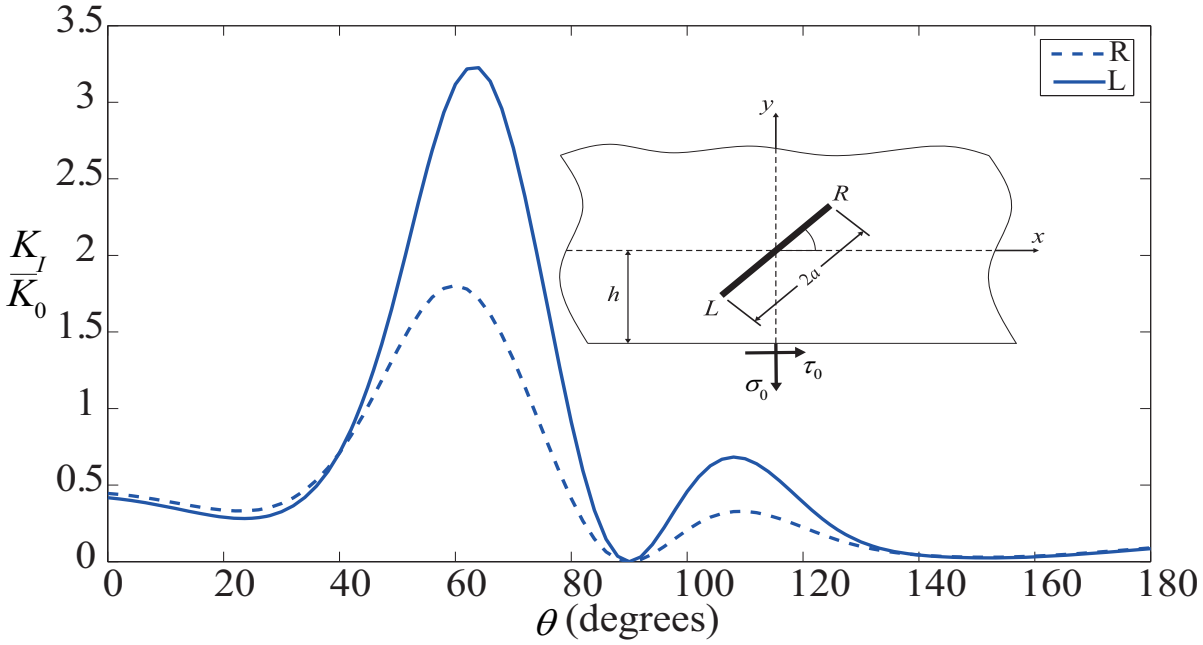

Figure 3b Non-dimensional mode I stress intensity factors for an oblique crack under normal and shear point loads.

In addition, the effect of shear traction on mode I can be seen in Figure (3b). According to the provided results, the shear traction highly effects the stress intensity factors and declines the SIFs values. In Figure (4), the effects of normal and shear loadings on the mode II can be seen. It is clear that the lack of geometric symmetry of cracks produces mode II SIFs even when cracks are subjected to normal traction Figure (4a). As can be seen, the mode II SIFs are increased and then declined dramatically at the vertical position. The SIFs allocate the least values at this position. It should be mentioned that as opposed to mode II, mode I is the dominant mode when $\theta = 0$ and stress intensity factor is far more than those of the mode II.

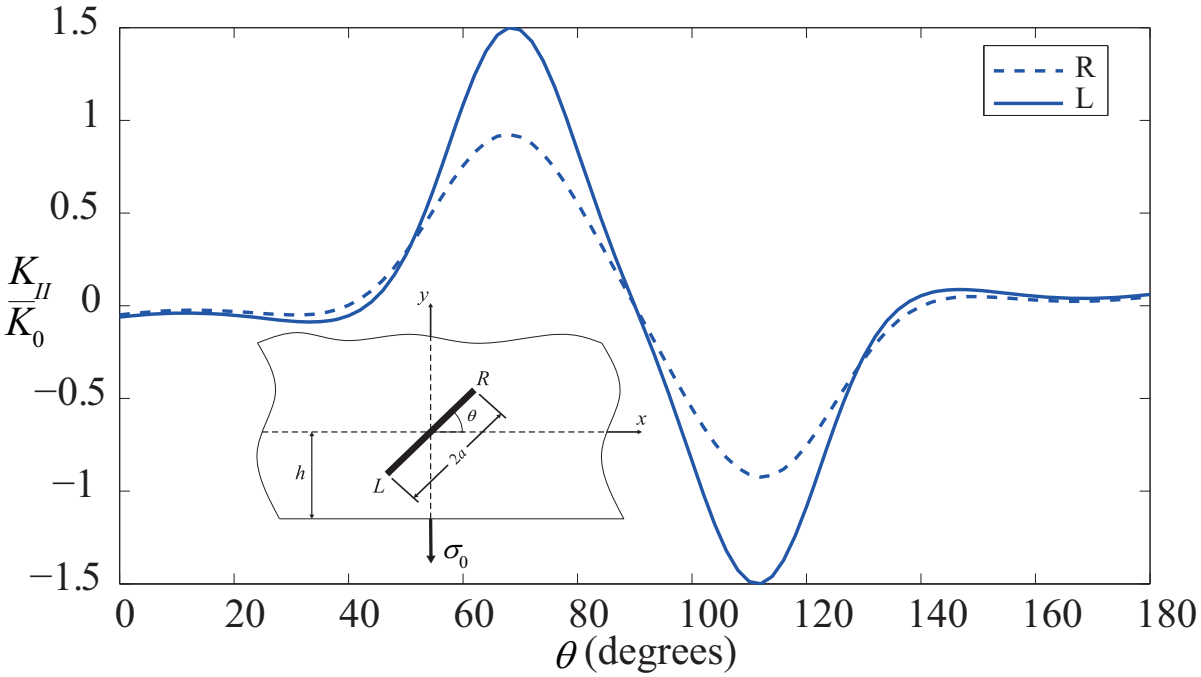

Figure 4a Non-dimensional mode II stress intensity factors for an oblique crack under normal point load.

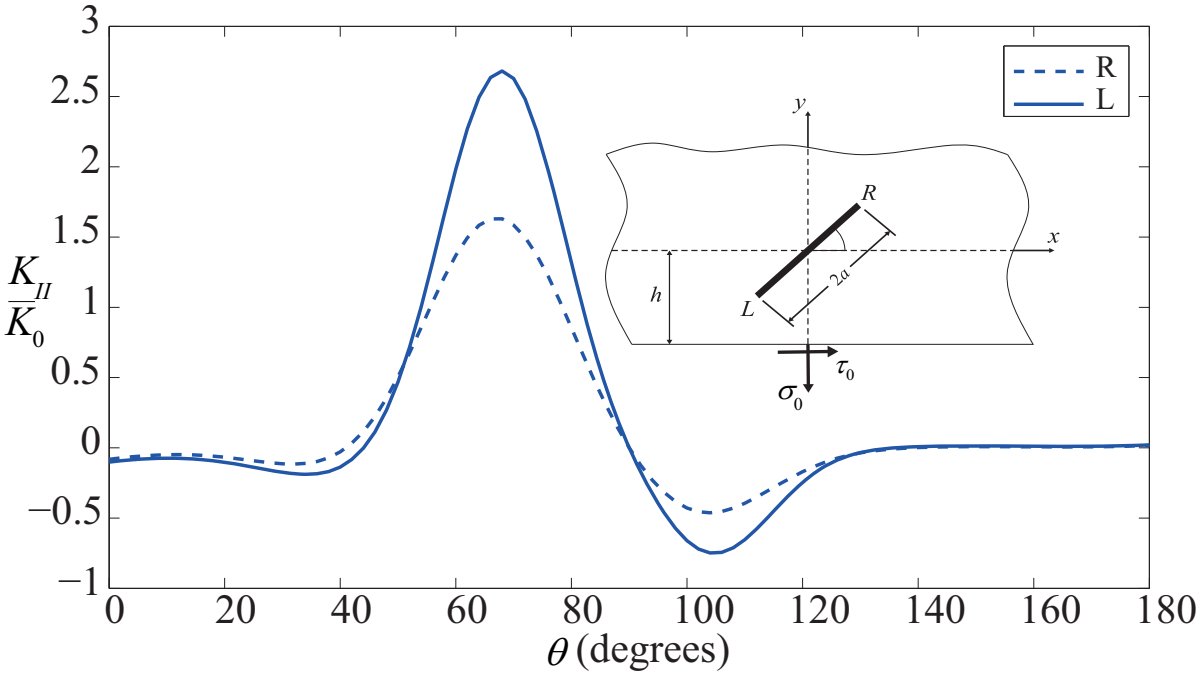

Figure 4b Non-dimensional mode II stress intensity factors for an oblique crack under normal and shear point loads.

In the second example, the interaction between two identical collinear cracks with the same lengths (Figures 5 and 6) subjected to normal mechanical point load are studied. The centers of cracks are fixed while the cracks lengths are changing with the same rate. As it was expected, due to the symmetry of cracks, the counterpart crack tips have the same SIF values. Besides, the values of mode I SIF increase as long as the length of the crack increases. The SIF for crack tips R_1 and L_2 increases dramatically which roots in the intense interaction between them. Furthermore, the mode II SIFs are considerably less than the mode I SIFs.

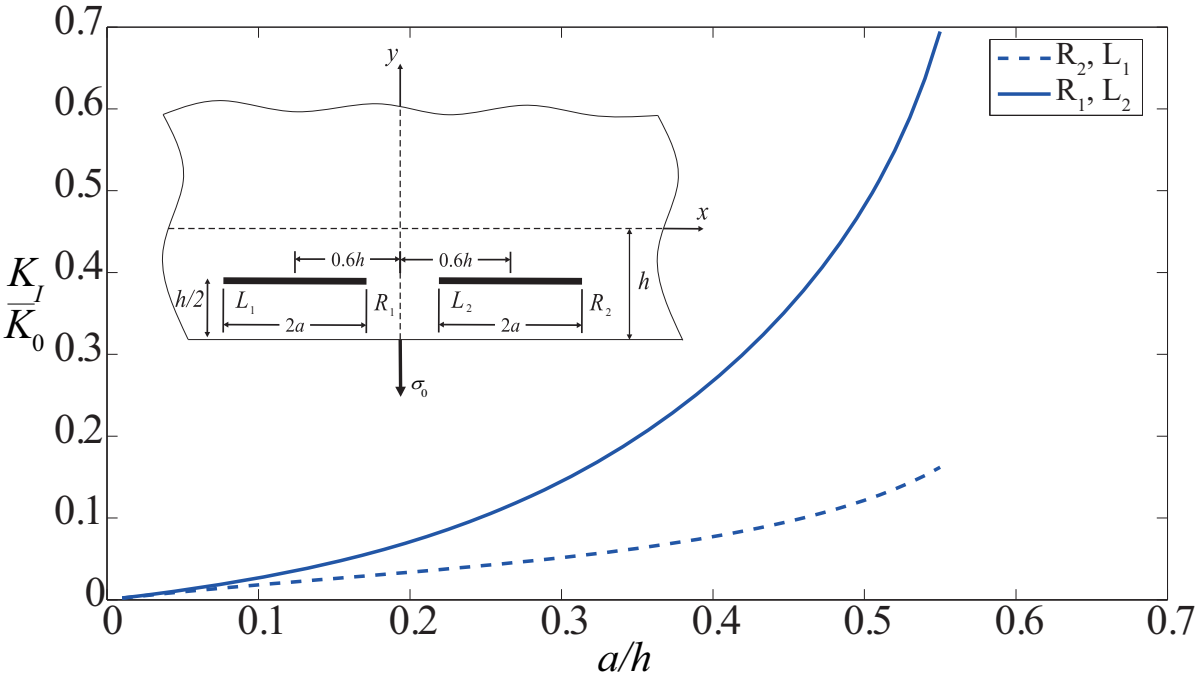

Figure 5 Non-dimensional mode I stress intensity factors for two collinear cracks.

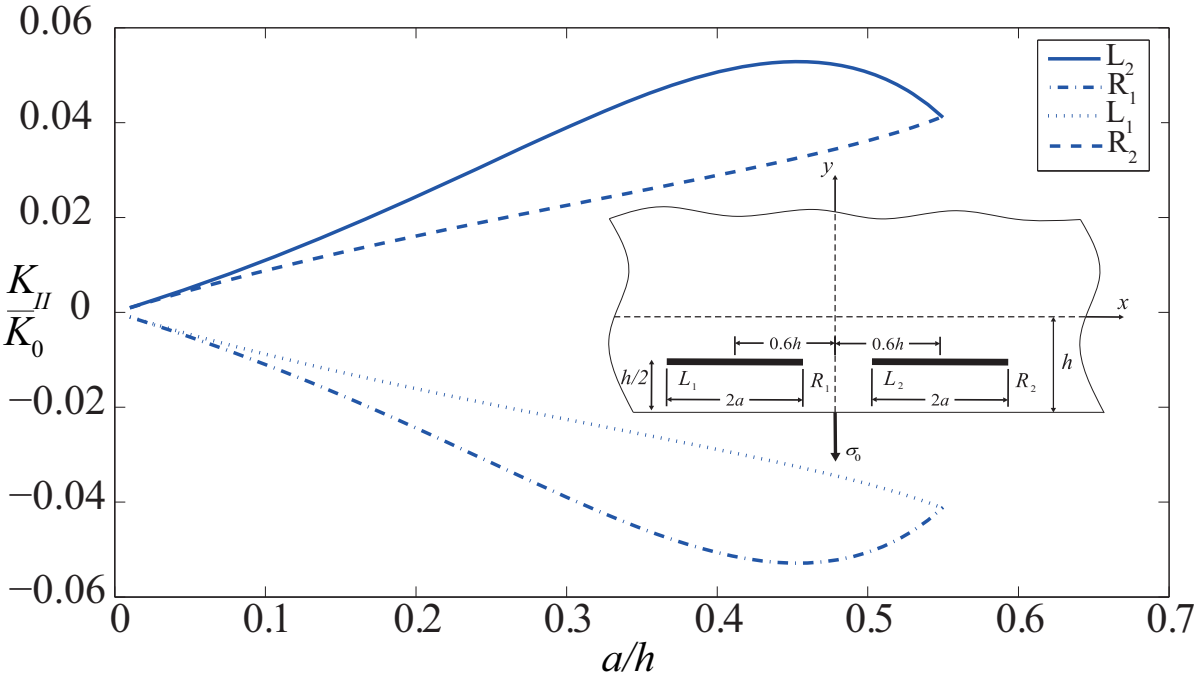

Figure 6 Non-dimensional mode II stress intensity factors for two collinear cracks.

In the next example, we consider two offset equal-length cracks parallel to the boundary of half-plane (see Figures 7 and 8). The variation of dimensionless stress intensity factors K_I/K_0 and K_{II}/K_0, are presented in Figures (7) and (8), respectively. As it was expected, the highest K_I/K_0 occurs where the distance between the interacting crack tips R_1 and L_2 is minima which indicates that the interaction between the crack tips increases. It is also found that the value of mode I and mode II SIFs grow steadily as long as the dimensionless crack length increases.

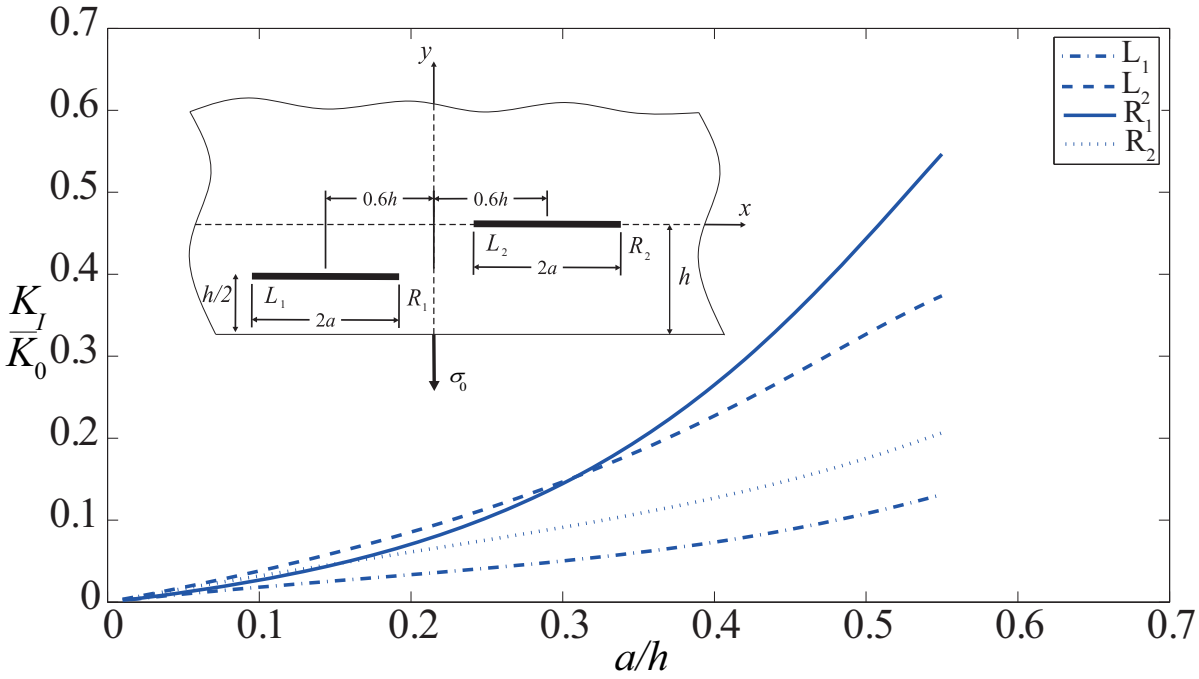

Figure 7 Non-dimensional mode I stress intensity factors for two parallel cracks.

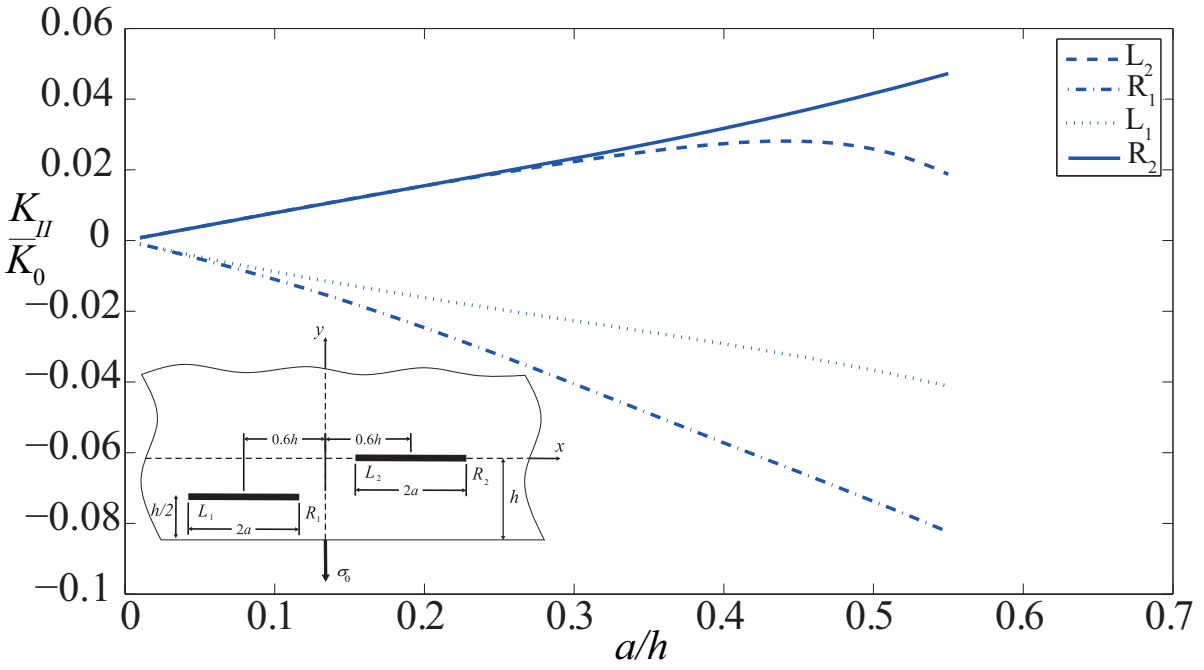

Figure 8 Non-dimensional mode II stress intensity factors for two parallel cracks.

Next, the half-plane is assumed to be weakened by a horizontal and an inclined crack, shown in Figures (9) and (10). It is assumed that the distance between the centers of the cracks is $2c = 1.5h$ which are situated symmetrically with respect to *y*-axis. It can be seen that the angle of crack orientation has a considerable effect on the mode I and mode II stress intensity factors; the SIFs for the rotating crack decreases as θ increases and then rises again. Furthermore, the SIFs of the rotating crack have the same values while θ is 0 and 180 degree due to symmetry.

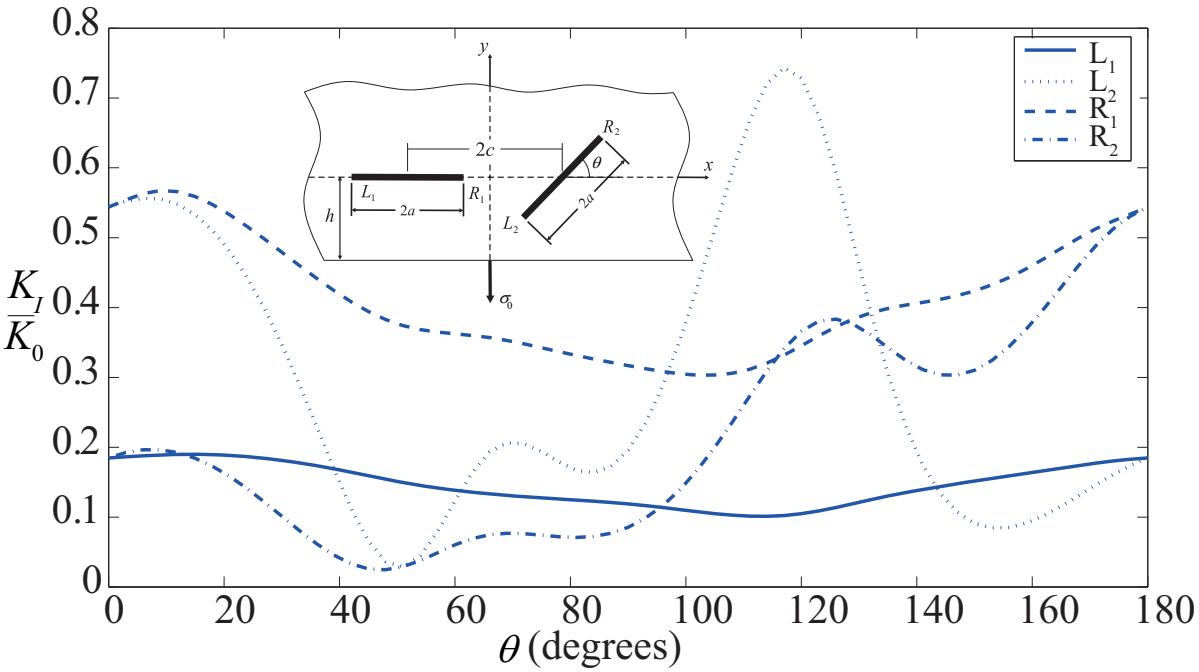

Figure 9 Non-dimensional mode I stress intensity factors for a fixed and oblique crack.

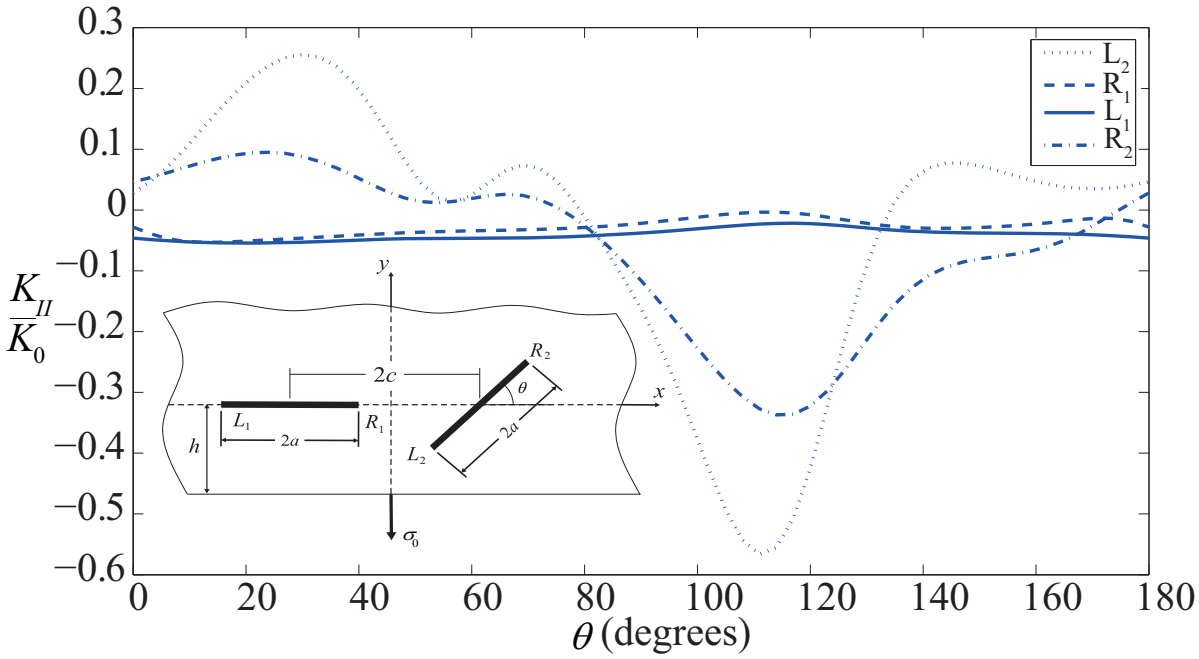

Figure 10 Non-dimensional mode II stress intensity factors for a fixed and oblique crack.

4.2 Medium under non-uniform thermal loading

In the following example, the effects of the non-uniform external thermal loading on the stress intensity factors are investigated. Here, it is assumed that there are no external in-plane mechanical loadings. The SIFs are normalized by $K_0 = \mu\alpha T_0\sqrt{a}$ and depicted in Figure (11). It is noticed that for mode I, the SIFs at tip L fluctuates as the crack length increases while the SIFs at tip R grows gradually. This is due to the fact that the applied non-uniform temperature at the boundary produces both normal and shear stresses to the medium which causes non-

symmetrical results. Moreover, it is observed that by doubling the parameter γ, the SIFs values decline significantly. On the other hand, the results shown in Figure (12) depicts that the second mode SIFs decrease steadily as long as crack length increases. It can be seen that by increasing the parameter γ the average values of K_{II} increases and then decreases as dimensionless crack length rises above 0.6.

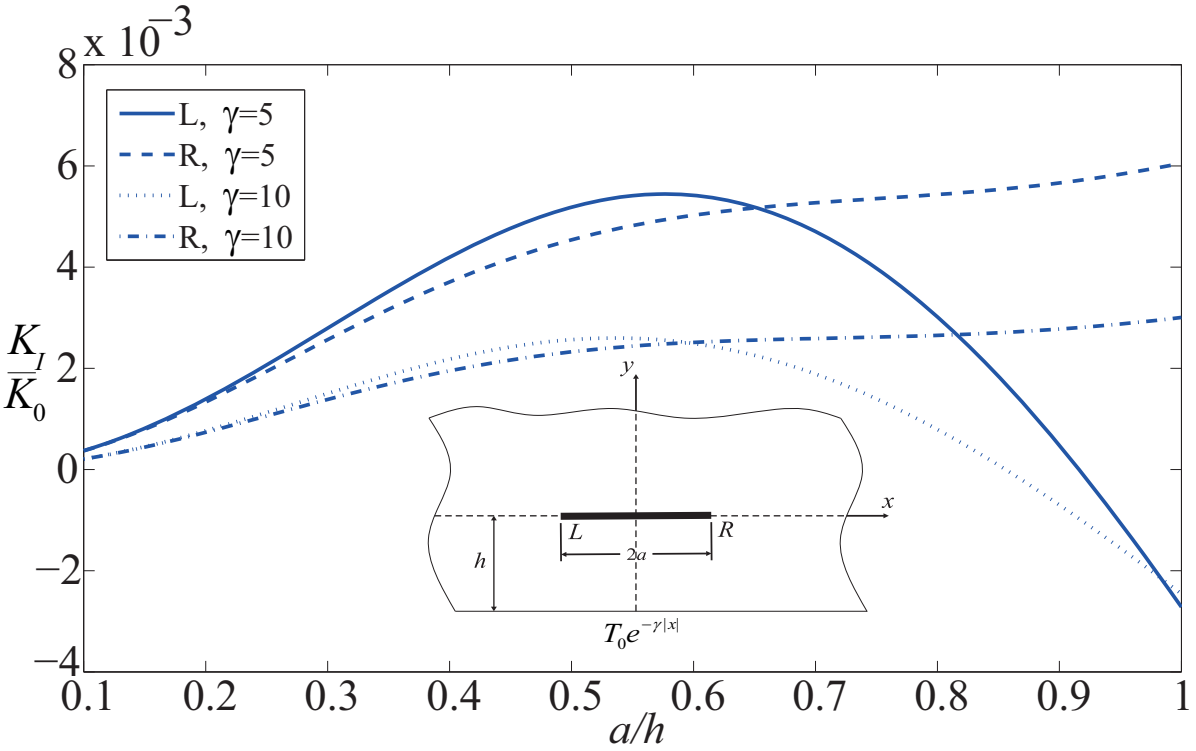

Figure 11 Mode I stress intensity factor versus crack length under thermal loading.

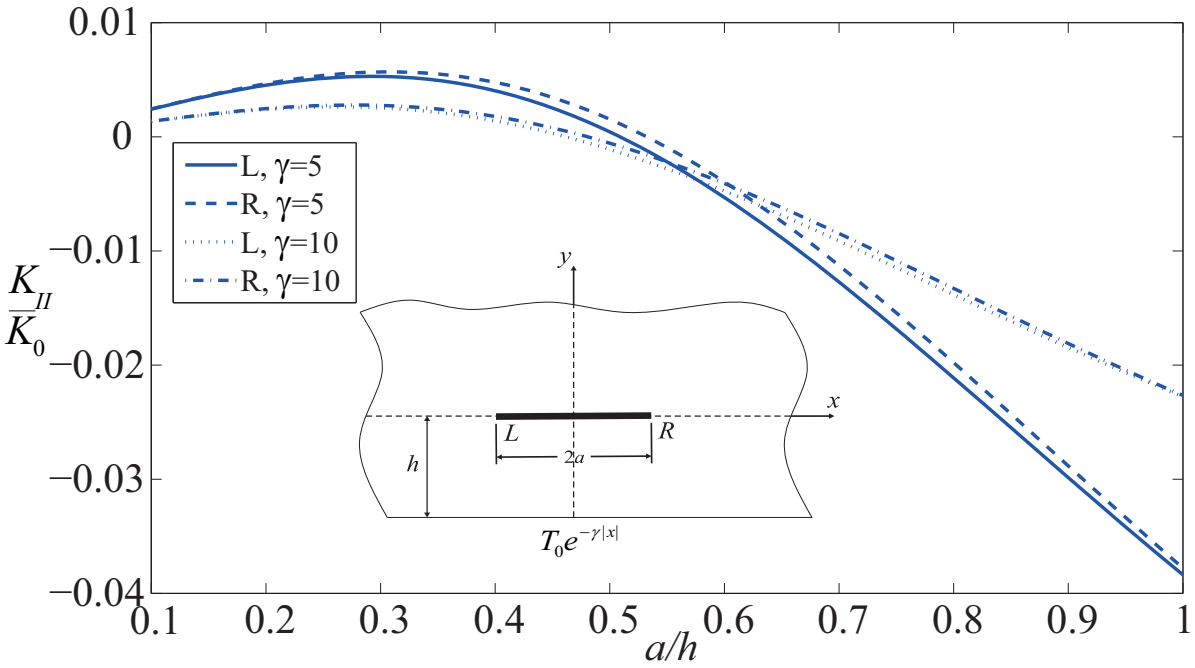

Figure 12 Mode II stress intensity factor versus crack length under thermal loading.

Furthermore, the effects of two collinear crack lengths on the stress intensity factors under non-uniform thermal loading is studied. According to the Figures (13a) and (13b), the mode I SIFs for two collinear cracks rises gradually as crack length increases. As expected, the interaction between crack tips R_1 and L_2 is far more than the two other crack tips.

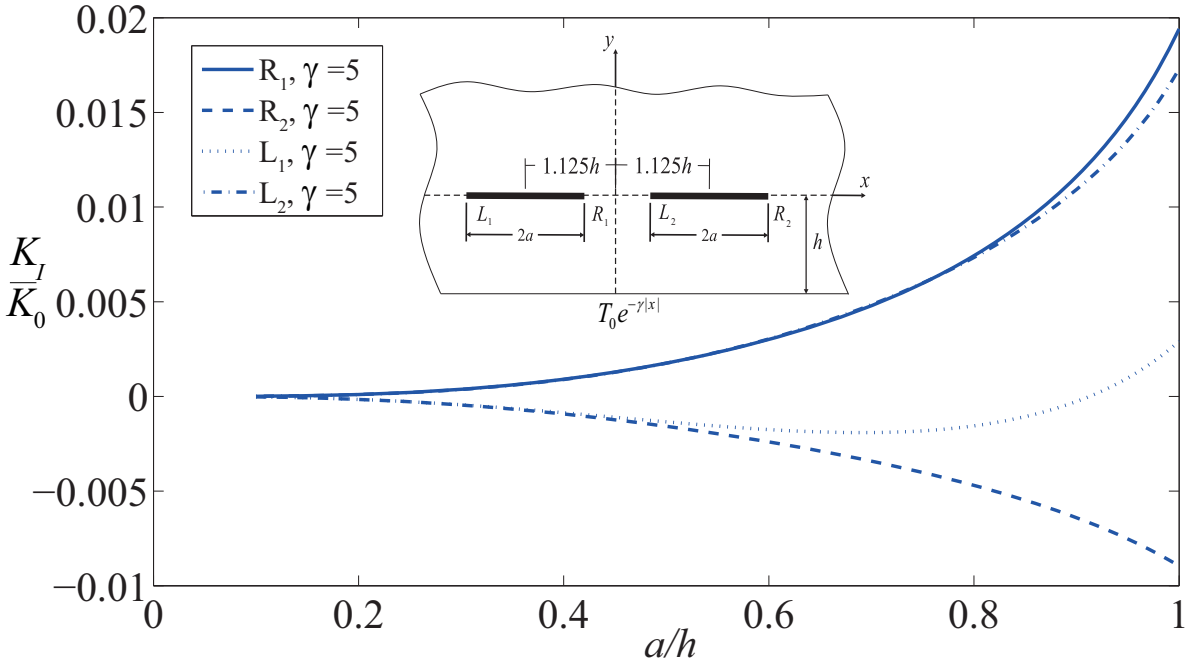

Figure 13a Mode I stress intensity factor for two collinear cracks under thermal loading for $\gamma = 5$.

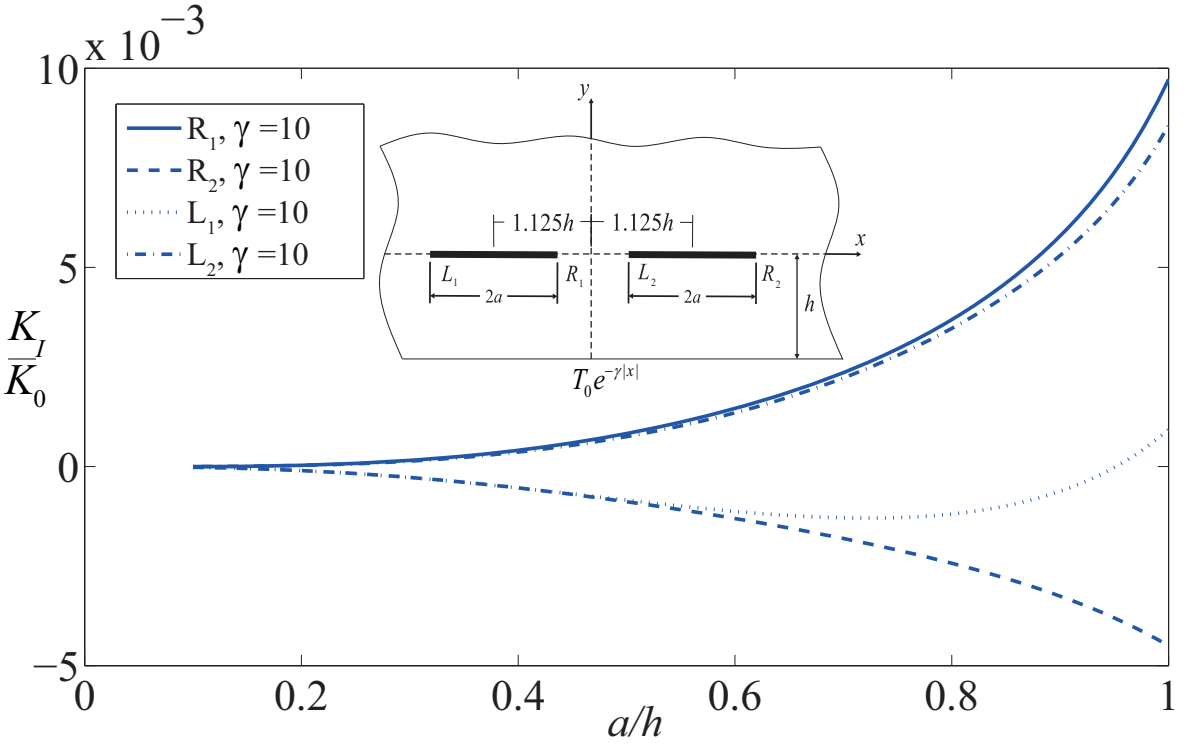

Figure 13b Mode I stress intensity factor for two collinear cracks under thermal loading for $\gamma = 10$.

Also, the given results in Figures (14a) and (14b) show an upward trend for second mode SIFs as crack length increases. It is noted that R_1 and L_2 possess considerably higher stress concentrations as crack length increases and, as a result, the interaction between two cracks rises significantly. In addition, the results depict that the effect of parameter γ on the SIFs is significant; by increasing the parameter γ, the amount of SIFs decreases.

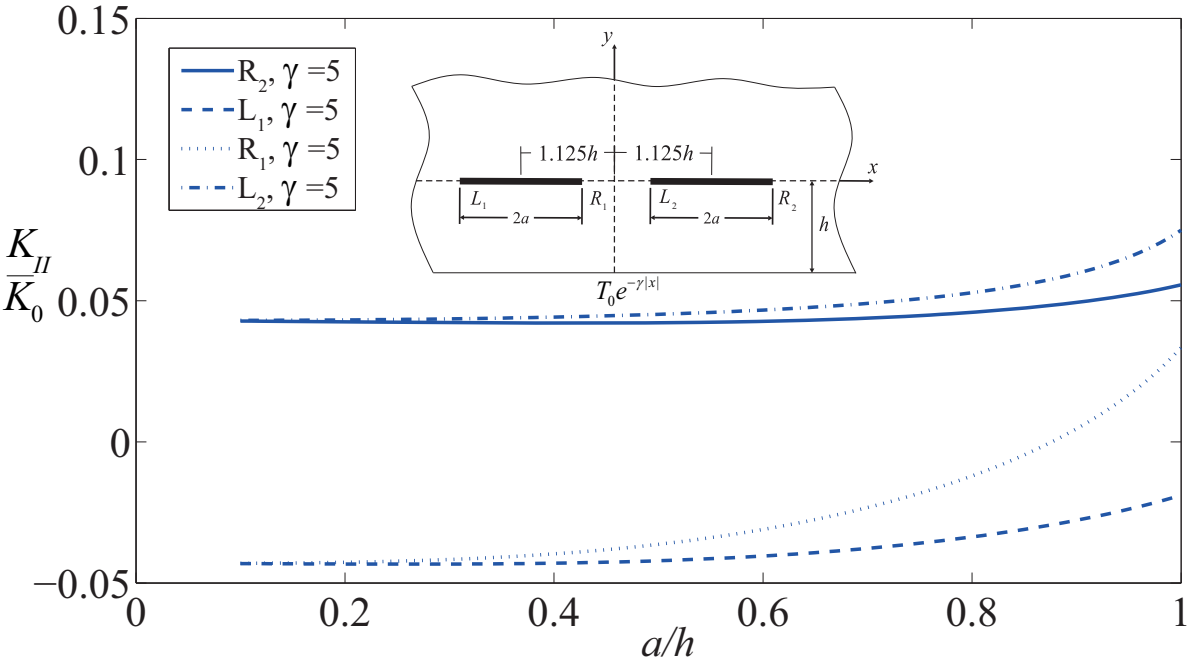

Figure 14a Mode II stress intensity factor for two collinear cracks under thermal loading for $\gamma = 5$.

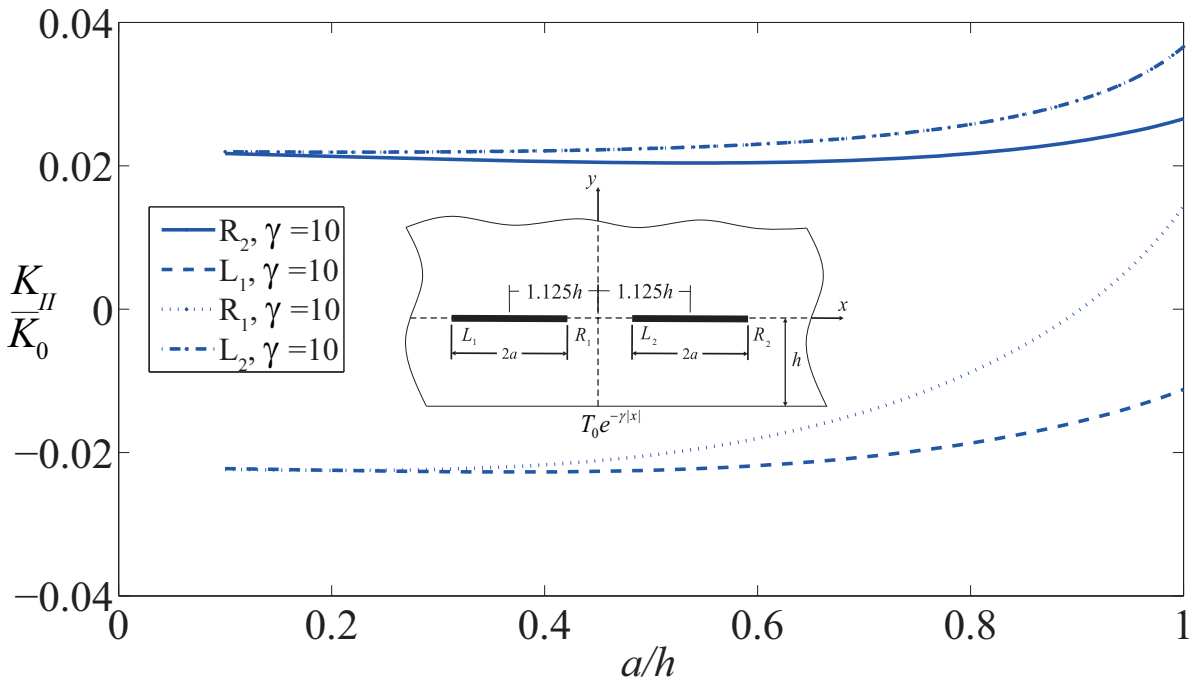

Figure 14b Mode II stress intensity factor for two collinear cracks under thermal loading for $\gamma = 10$.

4.3 Medium under thermo-mechanical loading

In this example the medium is considered to be under both in-plane mechanical and thermal loadings in which $T_0 = 100\,^{\circ}C$ and $\gamma = 5(1/m)$. The effect of crack length on the SIFs are demonstrated in Figures (15) and (16). The SIFs values rise as crack length increases. Additionally, it can be seen that SIFs for crack tips R and L is slightly more than the other tip for mode I and mode II, respectively.

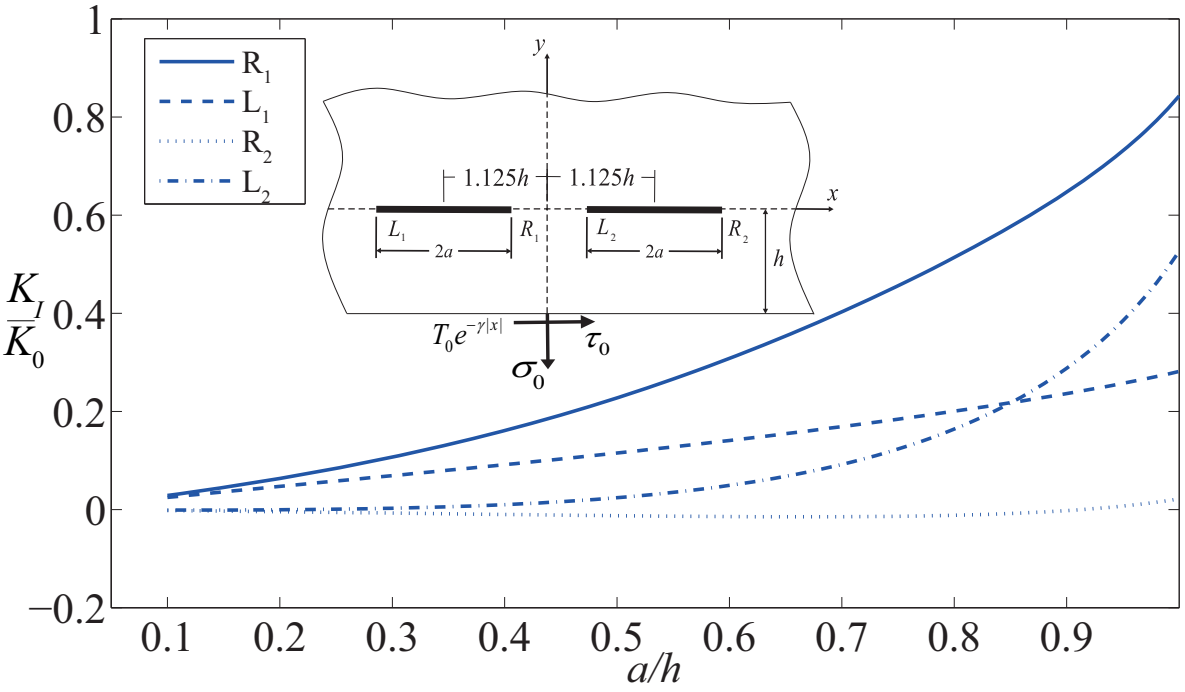

Figure 17 Mode I stress intensity factor for two collinear cracks under thermo-mechanical loading**.**

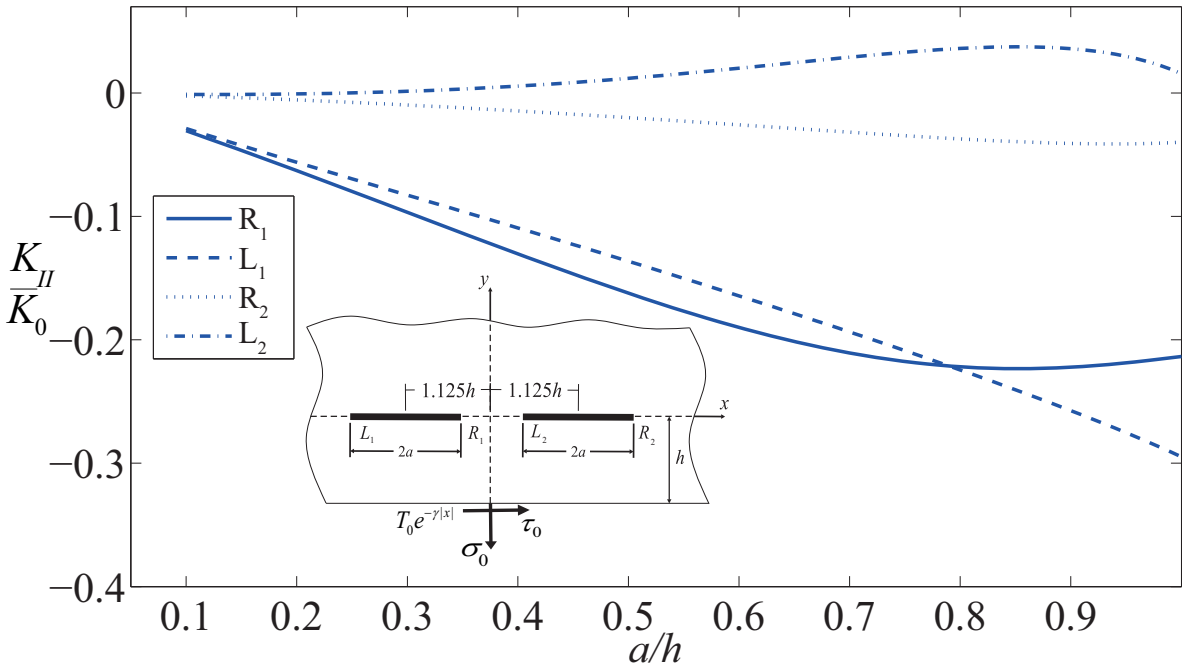

Figure 18 Mode II stress intensity factor for two collinear cracks under thermo-mechanical loading.

For the same loading, the interactions of two collinear horizontal cracks are studied in Figures (17) and (18). It can be seen that the first mode SIFs of both cracks rise steadily as long as crack length increases. The crack tip R_1 allocates considerably more SIF. Moreover, the Figure (18) illustrates that K_{II} increases by increasing the cracks length. It also shows that the SIFs for crack tips R_1 and L_2 increases considerably due to the significant interaction occurring between these two crack tips.

5 Conclusions

This paper investigates the steady state thermoelastic crack problem of a half-plane subjected to thermomechanical loading. The analytical closed-form solution of thermoelastic dislocation is obtained in the half-plane. For an arbitrarily located mechanical point load and external temperature load, fundamental solutions are derived. Then, the obtained solutions are utilized to obtain integral equations to formulate the behavior of cracks within the half-plane. These equations are of Cauchy singular type and are numerically solved to obtain dislocation density on the cracks surfaces. The crack surface is under traction-free conditions and the uniform heat flow is given vertically to the crack from the boundary. Several examples including single and multiple cracks under thermomechanical loadings are studied. The obtained formulation determines the cracks stress intensity factors of the weakened half-plane. This formulation can successfully be employed to analyze and design the cracked half-planes.

References

[1] Kovalenko, A.D., "*Thermoelasticity Basic Theory and Applications*", Wolters-Noordhoff, (1970).

[2] Sih, G.C., "On the Singular Character of Thermal Stresses Near a Crack Tip", Journal of Applied Mechanics, Vol. 29, pp. 587-589, (1962).

[3] Sekine, H., "Thermal Stresses Near Tips of an Insulated Line Crack in a Semi-infinite Medium under Uniform Heat Flow", Engineering Fracture Mechanics, Vol. 9, pp. 499-507, (1977).

[4] Atkinson, C., and Clements, D.L., "On Some Crack Problems in Anisotropic Thermoelasticity", International Journal of Solids and Structures, Vol. 13, pp. 855-864, (1977).

[5] Sturla, F.A., and Barber, J.R., "Thermal Stresses Due to a Plane Crack in General Anisotropic Material", Journal of Applied Mechanics, Vol. 55, pp. 372-376, (1988).

[6] Sturla, F., and Barber, J., "Thermoelastic Green's Functions for Plane Problems in General Anisotropy", ASME, Transactions, Journal of Applied Mechanics, Vol. 55, pp. 245-247, (1988).

[7] Noda, N., and Zhi-He, J., "Thermal Stress Intensity Factors for a Crack in a Strip of a Functionally Gradient Material", International Journal of Solids and Structures, Vol. 30, pp. 1039-1056, (1993).

[8] Jin, Z. H., and Noda, N., "An Internal Crack Parallel to the Boundary of a Nonhomogeneous Half Plane under Thermal Loading", International Journal of Engineering Science, Vol. 31, pp. 793-806, (1993).

[9] Jin, Z. H., and Noda, N., "Edge Crack in a Nonhomogeneous Half Plane under Thermal Loading", Journal of Thermal Stresses, Vol. 17, pp. 591-599, (1994).

[10] Erdogan, F., and Wu, B.H., "Crack Problems in FGM Layers under Thermal Stresses", Journal of Thermal Stresses, Vol. 19, pp. 237-265, (1996).

[11] El-Borgi, S., Erdogan, F., and Hidri, L., "A Partially Insulated Embedded Crack in an Infinite Functionally Graded Medium under Thermo-mechanical Loading", International Journal of Engineering Science, Vol. 42, pp. 371-393, (2004).

[12] Lee, Y. d., and Erdogan, F., "Interface Cracking of FGM Coatings under Steady-state Heat Flow", Engineering Fracture Mechanics, Vol. 59, pp. 361-380, (1998).

[13] Itou, S., "Thermal Stresses around a Crack in the Nonhomogeneous Interfacial Layer between Two Dissimilar Elastic Half-planes", International Journal of Solids and Structures, Vol. 41, pp. 923-945, (2004).

[14] Zhou, Y.T., and Lee, K.Y., "Thermal Response of a Partially Insulated Interface Crack in a Graded Coating-substrate Structure under Thermo-mechanical Disturbance: Energy Release and Density", Theoretical and Applied Fracture Mechanics, Vol. 56, pp. 22-33, (2011).

[15] Choi, H.J., "Thermoelastic Problem of Steady-state Heat Flows Disturbed by a Crack at an Arbitrary Angle to the Graded Interfacial Zone in Bonded Materials", International Journal of Solids and Structures, Vol. 48, pp. 893-909, (2011).

[16] Rizk, A.E. F.A., "Convective Thermal Shock of an Infinite Plate with Periodic Edge Cracks", Journal of Thermal Stresses, Vol. 28, pp. 103-119, (2004).

[17] Rizk, A.E. F.A., "Periodic Array of Cracks in a Strip Subjected to Surface Heating", International Journal of Solids and Structures, Vol. 41, pp. 4685-4696, (2004).

[18] Rizk, A.E. F.A., "An Elastic Strip with Periodic Surface Cracks under Thermal Shock", International Journal of Engineering Science, Vol. 44, pp. 807-818, (2006).

[19] Nied, H.F., "Thermal Shock Fracture in an Edge-cracked Plate", Journal of Thermal Stresses, Vol. 6, pp. 217-229, (1983).

[20] Rizk, A.E. F.A., and Radwan, S.F., "Fracture of a Plate under Transient Thermal Stresses", Journal of Thermal Stresses, Vol. 16, pp. 79-102, (1993).

[21] Rizk, A.E. F.A., "A Cracked Plate under Transient Thermal Stresses Due to Surface Heating", Engineering Fracture Mechanics, Vol. 45, pp. 687-696, (1993).

[22] Chen, Z.T., and Hu, K.Q., "Thermo-elastic Analysis of a Cracked Half-plane under a Thermal Shock Impact using the Hyperbolic Heat Conduction Theory", Journal of Thermal Stresses, Vol. 35, pp. 342-362, (2012).

[23] Hu, K., and Chen, Z., "Thermoelastic Analysis of a Partially Insulated Crack in a Strip under Thermal Impact Loading using the Hyperbolic Heat Conduction Theory", International Journal of Engineering Science, Vol. 51, pp. 144-160, (2012).

[24] Liu, L., and Kardomateas, G.A., "Thermal Stress Intensity Factors for a Crack in an Anisotropic Half Plane", International Journal of Solids and Structures, Vol. 42, pp. 5208-5223, (2005).

[25] Ravandi, M., and Fariborz, S.J., "Thermo-elastic Dislocation with Application to Crack Problems", European Journal of Mechanics A/Solids, Vol. 38, pp. 115-128, (2013).

[26] Hetnarski, R.B., and Eslami, M.R., "*Thermal Stresses: Advanced Theory and Applications*", Springer, (2009).

[27] Erdélyi, A., and Bateman, H., "*Tables of Integral Transforms: Based, in Part, on Notes Left by Harry Bateman*", McGraw-Hill, (1954).

[28] Fotuhi, A.R., Faal, R.T., and Fariborz, S.J., "In-plane Analysis of a Cracked Orthotropic Half-plane", International Journal of Solids and Structures, Vol. 44, pp. 1608-1627, (2007).

[29] Fotuhi, A.R., and Fariborz, S.J., "Stress Analysis in a Cracked Strip", International Journal of Mechanical Sciences, Vol. 50, pp. 132-142, (2008).

[30] Erdogan, F., Gupta, G.D., and Cook, T.S., "Numerical Solution of Singular Integral Equations", in: G.C. Sih (Ed.) Methods of Analysis and Solutions of Crack Problems: Recent Developments in Fracture Mechanics Theory and Methods of Solving Crack Problems, Springer Netherlands, Dordrecht, pp. 368-425, (1973).

[31] Ashbaugh, N., "Stress Solution for a Crack at an Arbitrary Angle to an Interface", International Journal of Fracture, Vol. 11, pp. 205-219, (1975).

Nomenclature

b_x, b_y	Burgers vector
B_{li}	Dislocation densities
$g_{li}(t)$	Regular terms of dislocation densities
h	Distance of the origin from the edge
$H(..)$	Heaviside step function
k_{ij}^{m}	Kernels of integral equations
K_0	Stress intensity factor of a crack in infinite plane
K	Thermal conductivity

K_{IL}, K_{IR}	Mode I stress intensity factor of crack tips
K_{IIL}, K_{IIR}	Mode II stress intensity factor of crack tips
N	Total number of cracks
u, v	The displacement fields
Q_n	Heat flux
$T(x, y)$	Temperature field
$\alpha_i(\eta), \beta_i(\eta)$	Functions describing the geometry of cracks
$\sigma_{ij}(x, y)$	The in-plane stress components
$\delta(..)$	Dirac delta function
θ_k, $k \in \{i, j\}$	The angle between *s*- and *x*-axes.
ζ	Fourier variable
$\varphi(x, y)$	Airy stress function

Appendix

The coefficients of Burgers vectors in Eq. (19) are expressed as:

$$\begin{aligned}
P_x &= f_x + 32h^5x + 64h^4xy + 28h^2xy(x^2+y^2) + xy(x^2+y^2)^2 \\
&\quad + 8h^3x(3x^2+7y^2) + 4hx(x^4+3x^2y^2+2y^4) \\
P_y &= 32h^5x + 64h^4xy + 4h^2xy(x^2+y^2) - 4hxy^2(x^2+y^2) \\
&\quad - xy(x^2+y^2)^2 + 8h^3x(x^2+5y^2) \\
P_{xy} &= f_{xy} - 32h^6 - 96h^5y - y^2(x^2+y^2)^2 - 32h^4(x^2+4y^2) - 32h^3(2x^2y+3y^3) \\
&\quad - 6h^2(x^4+8x^2y^2+7y^4) - 2h(3x^4y+8x^2y^3+5y^5)
\end{aligned} \tag{A.1}$$

$$f_x = (x^2 + (y+2h)^2)\int_0^\infty \frac{2e^{-\xi(y+2h)}}{\xi}\sin(\xi x)d\xi$$

$$f_{xy} = (x^2 + (y+2h)^2)\int_0^\infty \frac{e^{-\xi(y+2h)}}{\xi}\cos(\xi x)d\xi \tag{A.2}$$

$$\begin{aligned}
M_x &= -32h^5 - 96h^4y - 3x^4y - 4x^2y^3 - y^5 - 8h^3(x^2+13y^2) \\
&\quad - 4h^2(3x^2y+13y^3) - 4h(2x^4+3x^2y^2+3y^4) \\
M_y &= 32h^5 + 64h^4y - 8h^3(3x^2-5y^2) + 4h^2y(-9x^2+y^2) + y(x^4-y^4) - 4h(3x^2y^2+y^4) \\
M_{xy} &= 32h^4x + x^5 + 64h^3xy - xy^4 - 4h^2x(x^2-9y^2) + hx(-4x^2y+4y^3) \\
N_x &= x^5 - 32h^3xy - xy^4 + 4h^2x(5x^2-9y^2) + 12hxy(x^2-y^2) \\
N_y &= 96h^4x + x^5 + 192h^3xy + 4x^3y^2 + 3xy^4 + 12hxy\left(x^2+3y^2\right) + 12h^2x\left(x^2+11y^2\right) \\
N_{xy} &= -32h^5 - 96h^4y + 8h^3(3x^2-13y^2) + 12hy^2(x^2-y^2) + 4h^2(9x^2y-13y^3) + y(x^4-y^4)
\end{aligned} \tag{A.3}$$

چکیده

در این مقاله حل تحلیلی نابجایی ترموالاستیک در یک نیم صفحه الاستیک با استفاده از تبدیل فوریه بدست آمده است. سپس به کمک روش توزیع نابجایی مجموعه معادلات انتگرالی با تکینگی های کوشی برای محیط حاوی چندین ترک تحت بار حرارتی - مکانیکی بدست آمده است. با حل عددی معادلات انتگرالی و محاسبه دانسیته های نابجایی بر روی سطوح ترک ها، از آن برای محاسبه ضرایب شدت تنش مکانیکی و حرارتی استفاده شده است. نتایج عددی برای مودهای یک و دو مکانیک شکست ارائه شده است در نهایت اثر هندسه ترکها شرایط بارگذاری بر روی ضرایب شدت تنش بدست آمده است.